Investigation into the behaviour of an iced low Reynolds number aerofoil

N.L.Oo*, N.J.Kay, A.J.Brenkley and Dr R.N.Sharma
University of Auckland, Khyber Pass Rd, Auckland, New Zealand

ABSTRACT

Icing is a known hazard and has contributed to air accidents through its increased weight and reduced aerodynamic performance. A small UAV is more vulnerable to icing as it cannot afford the mass and power of de-icing systems, and, due to their small size, the added mass is proportionally greater. Compounding this are the effects of low Reynolds number flows.

To determine the impact of ice on a small UAV, a wind tunnel study was conducted with four ice shapes attached to the wing of a Kahu UAV at a Reynolds number of 200,000. Computational Fluid Dynamics (CFD) simulations to determine the change in stall behaviour. In all the cases, the ice accretion increased drag considerably, but the lift coefficient was altered for only one bluff-formed ice shape.

1 INTRODUCTION

Wing icing and the associated performance degradation is a known hazard for manned aircraft, being highlighted as the primary cause of notable crashes such as the loss of an ATR-72-212 over Roselawn, Illinois [1]. In flight wing icing forms as a result of supercooled water droplets in the air contacting the cold wing surface and freezing [2]. The form in which the ice freezes depends not only on the air temperature, but the amount of moisture in the air, the size of the water droplets, the relative speed of the wing, the wing leading edge radius and angle of attack.

Ice can form as one of three types. Rime is white and rough, while, glaze is clear, solid and smooth. Mixed consists of a combination of both. While rime ice remains close to the aerofoil form, glaze may form horns at the leading edge [3], significantly altering the aerofoil form. This change in geometry alters the associated forces and moments. Additionally, a significant mass is added to the airframe, increasing the demand on both engine and aerofoil and increasing surface roughness increases drag.

To counter this, manned aircraft designed to operate in potential icing conditions must be certified with appropriate de-icing equipment. For a small UAV, this is not a viable option. A small UAV is typically hand-launched, below 5kg, and so cannot afford the weight or power penalty associated with de-icing methods. Furthermore, the mass of the ice is proportionally more of the airframe weight [4] due to the low initial mass. The required excess power to counter the added mass may result in a much reduced endurance, or potentially result in loss of the aircraft.

Compounding this is the fact that small UAVs fly at low Reynolds numbers, typically below 250,000, due to their small size and low speed. This flow regime is dominated by a laminar and transitional boundary layer, with performance highly dependent on the behaviour of the Laminar Separation Bubble (LSB). This is a region of separated and recirculating flow, where the laminar boundary layer has detached from the aerofoil surface, but is able to reattach via transitioning to a turbulent flow and the enhanced momentum entrainment. The size of this bubble strongly influences lift and drag, and

*contact email: noo122@aucklanduni.ac.nz

depends on many parameters, but most importantly on the Reynolds number, Adverse Pressure Gradient (APG), upstream flow disturbances and surface roughness [5]. Increasing the Reynolds number, roughness and freestream disturbances will typically decrease the LSB size by accelerating transition, while increasing the APG provides the opposite effect. Hence, the addition of roughness due to ice may even aid aerofoil lift performance due to the reduced LSB size, at the cost of increased drag due to higher friction.

Prior emphasis has been on avoiding potential icing conditions [6], significantly limiting the operational utility of small UAVs. In order to assess the effect of ice on a small UAV in cruising flight, sampled ice shapes were mounted to the leading edge of a small UAV wing and physically tested. The aim was to assess the changes in the steady-state lift, drag and pitch moment coefficients at cruise. Additionally, CFD simulations were undertaken to provide more detailed flow assessment and visualisation for key test cases, to understand the changes in aerodynamic behaviour.

2 METHODOLOGY

2.1 Physical Testing

The initial phase of this study was conducted using the wing from a small Kahu UAV. Kahu is a fixed-wing UAV with a 2 m wingspan, which flies at approximately 60 km h^{-1}, or a Reynolds number of 230,000. This wing was mounted on the six-axis force balance of the Twisted Flow Wind Tunnel (TFWT) at the University of Auckland (UoA).

It was desired to assess the change in the performance of the wing with differing ice accretion. Four ice shapes were provided by the National Research Council of Canada (NRC) [7, 8]. These were generated in the NRC High-Altitude Icing Wind Tunnel to the standard of FAR25 Appendix C [9], simulating a variety of icing conditions and formation Angles of Attack (AoA). The ice shapes were replicated via 3D-Printed using Fused-Deposition Modelling. The ice shapes generated by NRC displayed similar roughness to that seen by Shin [10], and hence further roughening was not employed.

These cross-sections are presented in Figure 1, with the red representing the outer ice form, and the blue the aerofoil leading edge. From left to right, the ice shapes are designated by their formation AoA and ice formation condition, where IM is Intermittent Maximum, equivalent to Cumuliform clouds at -20°C, while CM is Continuous Maximum, representing Stratiform clouds at -5°C.

Figure 1 – Ice Shape Cross-Sections [7, 8]

Testing was conducted at a Reynolds number of 200,000 based on the mean wing chord. The freestream turbulence intensity was measured to be 1.1%, with a floor boundary layer depth of 400 mm. For this reason, the wing was mounted in the vertical orientation 520mm above the floor level, a splitter plate providing a reference plane at the wing root. Data was gathered from -4° to 20°, covering typical flight attitudes.

Data was gathered solely through the force balance, as the wing could not be modified. The force and torque loads of the mount were measured and subtracted from all the data. The force balance resolution was 0.05 N for forces and 0.1 Nm for moments [11]. As the force resolution was over an order of magnitude lower than the lowest drag coefficient anticipated for the clean aerofoil per the data of Selig et al. [12], this was sufficient for the measurement of this data. The pitch moment resolution, however, was comparable to the data expected, and so can only be seen as a reference trend. As the force balance

is not configured for high-frequency acquisition, time-averaged coefficients were derived.

2.2 CFD

The stall behaviour of the clean aerofoil and the 0° IM ice shape were investigated further via CFD. The turbulence model employed was Scale-Adaptive Simulation-Shear-Stress Transport (SAS-SST). This is an Unsteady Reynolds-Averaged Navier-Stokes (URANS) model, based on the SST formulation for low-cost solving where the flow is stable. However, unlike basic SST, SAS-SST adjusts its source terms, allowing it to simulate large-scale flow structures, such as those in the wake of a stalled aerofoil, in a manner comparable to Large Eddy Simulation (LES) [13]. The capability of the SAS-SST in the wake region was proven by Garbaruk et al. [14], with the numerical results comparable to the experiment.

A C-grid configuration was used, maintaining an inlet three chord lengths upstream of the clean wing leading edge, and an outlet opening five chords downstream. This was based on a prior LES study on aerofoils in similar flow conditions [15]. Symmetry planes were used to enforce a two-dimensional set-up to focus on the aerofoil behaviour in isolation of wing effects. Free-slip wall boundary conditions at the top and bottom of the domain were kept at a reasonable distance, so as not to have any influence on the solution.

The compact domain allowed for a high mesh density in proximity to the wing and its wake, as shown in Figure 2. The meshing was completed with a total of 383,298 elements using ANSYS ICEM-CFD. The wall normal mesh was kept at $\Delta y^+ < 1$ and the chordwise mesh resolution of $\Delta x^+ = 10$ over the ice accreted chord and $\Delta x^+ = 28$ at the downstream of the ice-shape. Although not as sensitive as LES, Egorov and Menter [16] demonstrated that energy dissipation is dependent on grid size, and so the use of an LES grid provided suitable resolution in the wake.

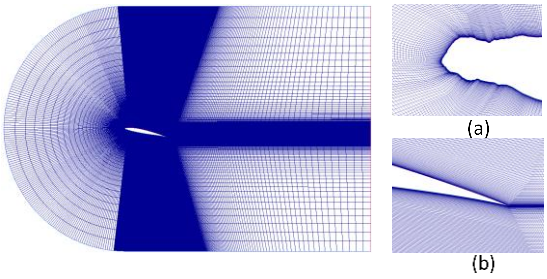

Figure 2 – 0° IM Aerofoil mesh at 14.5° AoA, with detail (a) leading-edge (b) trailing-edge

Simulations were run for five seconds with 5,000 time steps. The same time step of 0.001s, was set to the same for all of the simulations, enabling aerodynamic unsteadiness to be observed up to the maximum frequency of interest of 500 Hz.

3 RESULTS

3.1 Physical Testing

Figures 3 and 4 compare the aerodynamic performance of the test wing with each ice form and the baseline clean wing. Evident in Figure 3 is that the ice has no apparent impact on the lift coefficient below 10° AoA. While the form of the aerofoil is altered, reducing camber at the leading edge, this effect is countered by the added surface area, producing the same lift coefficient for the given reference clean wing planform.

Beyond 11° AoA, however, the ice shapes produce differing behaviour. The 0° IM ice shape most notably results in an earlier stall, with the corresponding reduced maximum lift coefficient. This is the most bluff-formed ice shape with a more sudden change in form. However, it also has the gentlest stall, suggesting a different stall mode from the other forms. In terms of flight operation, this early stall would suggest reduced AoA limits should be enforced when icing is present to maintain safe flight.

By comparison, the clean wing has the sharpest stall, with a gentle reduction followed by a sharp drop. This suggests a trailing-edge stall reaching the LSB and commencing full separation. The

remaining three ice shapes are similar in performance, with a higher maximum lift coefficient and later stall, which is slightly gentler than the clean aerofoil case. This is likely a result of flow instabilities generated by the ice, resulting in a higher energy boundary layer which thus remains attached longer.

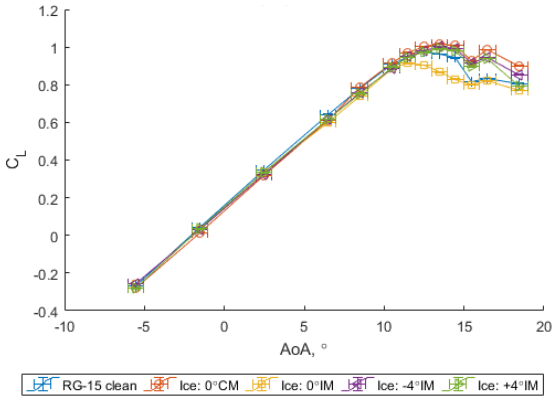

Figure 3 – Lift Coefficient against AoA

Similarly, Figure 4 shows an increased drag coefficient for the 0° IM ice shape for a given lift coefficient, with the exception of at lift coefficients between 0.6 and 0.8. In this region, the -4° IM ice shape has the highest drag. This is because the ice sits entirely on the upper surface of the leading edge, with its depth more exposed as AoA increases. As expected, the clean wing has the lowest drag at all AoA, and thus the lowest power requirements.

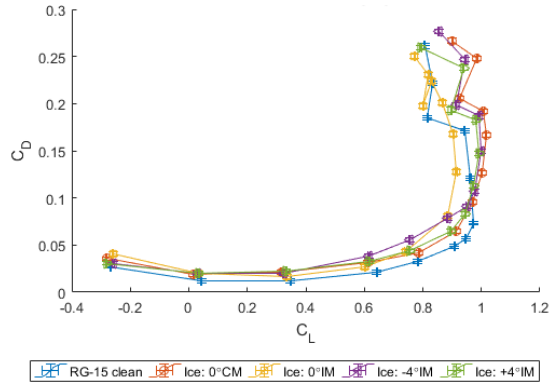

Figure 4 – Drag Coefficient against Lift Coefficient

Of note is that, for this UAV, the mass of the ice was estimated at 0.2 kg, approximately 10% of the UAV mass. This requires the AoA to be raised by 1°. Combined with the increased drag coefficient for a given AoA, this has a significant effect on endurance, potentially up to 50%.

3.2 Numerical Simulation

The CFD allows visual inspection of the difference in stall behaviour of the clean and 0° IM cases, and comparison of the pressure distributions. The selected AoA for assessment were 11.5° and 14.5°, corresponding to the stall AoA of the 0° IM and clean aerofoil, respectively. Figure 5 represents the velocity contours of clean and ice-accreted aerofoil at these AoA.

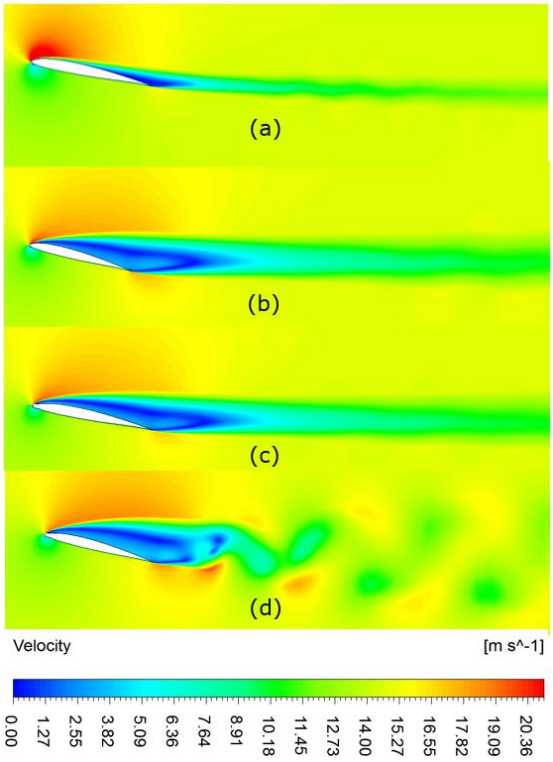

Figure 5 – Velocity contour plots (a) 11.5°, clean (b) 14.5°, clean (c) 11.5°, 0° IM (d) 14.5°, 0° IM

On the clean aerofoil, a short LSB was observed at around the leading-edge of the aerofoil at 11.5°, as seen in Figure 6. A large stagnant area is also seen towards the trailing edge in this condition in Figure 5. At 14.5°, this has reached the LSB and complete, but stable, separation ensues, which is the start of stall. In comparison, the bluff-edge 0° IM case has reached this state at the lower angle of 11.5°.

This is also reflected in Figure 7, with the 11.5° AoA, where the suction surface shows a similar C_p to that of the clean wing at 14.5°. In this case, the flow cannot reattach after separating on the blunt form of the ice. By 14.5°, the ice-accreted aerofoil shows the clearly defined vortex street seen in Figure 5, acting as a bluff-body separation. Of interest also are the small pressure pockets in the cavities of the ice on the pressure side.

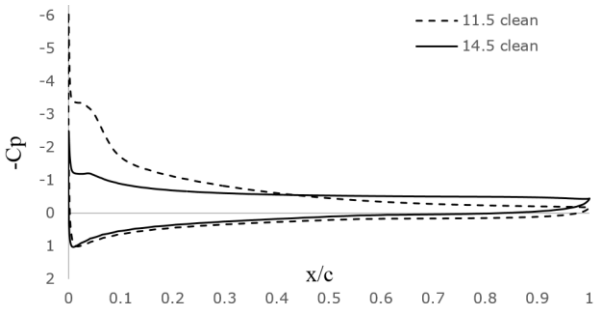

Figure 6 – Pressure coefficients comparison for clean aerofoil at 11.5° and 14.5°

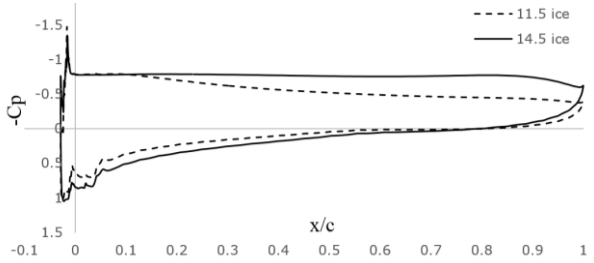

Figure 7 – Pressure coefficients comparison for ice-accreted aerofoil at 11.5° and 14.5°

Mirzaei et al. [17] observed that the fundamental vortex shedding frequency for ice-accreted aerofoil decreases with an increase in AoA, similar to a clean aerofoil. This was also observed in the CFD results, as shown in Figures 8 and 9, in which the velocity Power Spectral Densities (PSD) at a point in the wake, 2.5 chords downstream, are plotted. The fundamental frequency decreases from 69 Hz at 11.5° AoA to 55.6 Hz at 14.5° for the clean aerofoil. In the ice-accreted cases, however, the fundamental and secondary peaks were notably more prominent, while being only 4 Hz and 2 Hz lower for 11.5° and 14.5° AoA, respectively. This is a result of the greater vorticial energy provided by the rough ice form, maintaining time-averaged suction pressures and thus the gentler stall. In all the simulated cases, using the projected flow-normal aerofoil depth, the Strouhal numbers are in good agreement with that expected from bluff-body vortex shedding [18], being between 0.21 and 022.

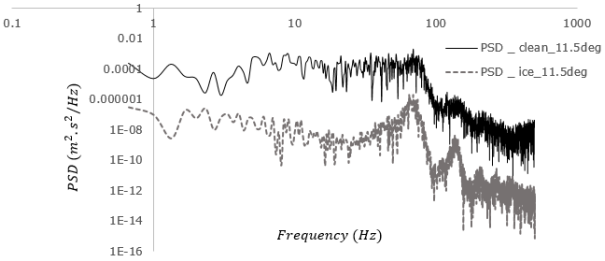

Figure 8 – Velocity PSD comparisons for clean and ice accreted aerofoil, 11.5° AoA. 0° IM is decreased by 3 orders of magnitude for clarity

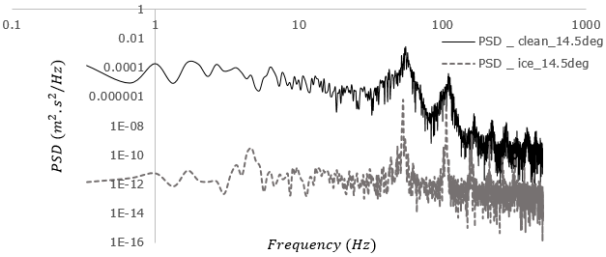

Figure 9 – Velocity PSD comparisons for clean and ice accreted aerofoil, 14.5° AoA. 0° IM is decreased by 6 orders of magnitude for clarity

4 CONCLUSIONS

The wind tunnel study showed that ice accretion does have a significant effect on UAV operation, primarily due to the increase in drag and so the corresponding loss of endurance. This would need to be accounted for in mission planning. The lift coefficient was only altered in one case, reducing the stall AoA to 11.5°. As such, when flying in icing conditions, the AoA envelope permitted should be reduced to account for a reduced stall tolerance, but lift capability is unaltered below this.

The CFD shows this change is attributed to the bluff form of the ice, which does not permit flow reattachment and hence no LSB is formed. The

amplitude of fluctuations is also greater, necessitating greater control response.

While the CFD in this study examined the high-AoA cases, given the increased fluctuation with the ice, it would be desirable to investigate fluctuations in the forces acting on the wing at low AoA, in normal cruise. This would assist in adapting control systems to be more robust when ice may be present. Furthermore, the effects of span should also be assessed, as turbulence is fundamentally three-dimensional.

ACKNOWLEDGEMENTS

The authors would like to extend their thanks to the NRC and the Defence Technology Agency of the New Zealand Defence Force for providing the physical test specimens, and the New Zealand eScience Infrastructure for use of their high-performance cluster for the simulations.

REFERENCES

[1] NTSB, "Aircraft Accident Report: In-flight Icing Encounter and Loss of Control," NTSB, NTSB/AAR-96, Washington D.C, 1994.

[2] National Weather Service, "Aircraft Icing," http://www.crh.noaa.gov/Image/lmk/Brian%20S/LMK_Icing_Show.pdf [cited December 17 2014].

[3] FAA, "Chapter 15: Ice and Rain Protection," https://www.faa.gov/regulations_policies/handbooks_manuals/aircraft/amt_airframe_handbook/media/ama_Ch15.pdf [cited March 25 2015].

[4] Szilder, K., and McIlwain, S., "In-flight icing of UAVs-the influence of flight speed coupled with chord size," *Canadian Aeronautics and Space Journal,* Vol. 58, No. 2, 2012, pp. 83-94.

[5] Gaster, M., "The structure and behaviour of laminar separation bubbles," Aeronautical Research Council, R&M No. 3595, London, UK, 1969.

[6] Siquig, R.,A., "Impact of Icing on Unmanned Aerial Vehicle (UAV) Operations," Naval Environmental Prediction Research Facility, PR 90:015:442, 1990.

[7] Brenkley, A., "Aerodynamic Performance of the Kahu UAV with Ice Formation on the wings at Low Reynolds Numbers," Part IV project report, 2015-ME14, 2015.

[8] Kay, N.J., "Aerodynamic Performance of the Kahu UAV with Ice Formation on the wings at Low Reynolds Numbers," University of Auckland, ME053-2015, Auckland, New Zealand, 2015.

[9] FAA, "Appendix C to Part 25," http://www.ecfr.gov/cgi-bin/text-idx?rgn=div5;node=14%3A1.0.1.3.11#ap14.1.25_11801.c [cited 19 September 2015].

[10] Shin, J., "Characteristics of Surface Roughness Associated With Leading Edge Ice Accretion," *AIAA 32nd Aerospace Sciences Meeting and Exhibit,* Vol. NASA TM-106459, AIAA, Reno, Nevada, 1994,

[11] Yacht Research Unit, "TFWT Specifications," http://homepages.engineering.auckland.ac.nz/~dpel004/yru/html/Wind-tunnel/ [cited March 21 2015].

[12] Selig, M.S., Guglielmo, J.J., Broeren, A.P., "Summary of Low-Speed Airfoil Data, Volume 1," SoarTech Publications, Virginia Beach, Virginia, USA, 1995,

[13] Menter, F.R., "Best practice: scale-resolving simulations in ANSYS CFD," *ANSYS Germany GmbH,* 2012, pp. 1-70.

[14] Garbaruk, A., Shur, M., Strelets, M., "NACA0021 at 60 deg. incidence," *Notes on Numerical Fluid Mechanics and Multidisiplinary Design,* Vol. 103, 2009, pp. 127-139.

[15] Itsariyapinyo, P., and Sharma, R., "NACA0015 Circulation Control Airfoil Using Synthetic Jets at Low Angles of Attack and Low Reynolds Number," *8th AIAA Flow Control Conference,* 2016, pp. 3772.

[16] Egorov, Y., and Menter, F., "Development and application of SST-SAS turbulence model in the DESIDER project," *Advances in Hybrid RANS-LES Modelling,* Springer, 2008, pp. 261-270.

[17] Mirzaei, M., Ardekani, M.A., and Doosttalab, M., "Numerical and experimental study of flow field characteristics of an iced airfoil," *Aerospace Science and Technology,* Vol. 13, No. 6, 2009, pp. 267-276.

[18] Yarusevych, S., Sullivan, P.E., and Kawall, J.G., "On vortex shedding from an airfoil in low-Reynolds-number flows," *Journal of Fluid Mechanics,* Vol. 632, 2009, pp. 245-271.